

Article

Ameliorative Effects of *Annona muricata* Leaf Ethanol Extract on Renal Morphology of Alloxan-Induced Mice

Supri Irianti Handayani ¹, Mutiara Intan Permata Sari ¹, Meilania Saraswati Sardjana ¹, Kusmardi Kusmardi ¹ , Siti Nurbaya ², Rosmalena Rosmalena ^{3,*}, Ernawati Sinaga ⁴ and Vivitri Dewi Prasasty ^{5,*}

¹ Department of Anatomic Pathology, Faculty of Medicine, Universitas Indonesia, Jakarta 10430, Indonesia

² Department of Clinical Pathology, Faculty of Medicine, Universitas Indonesia, Jakarta 10430, Indonesia

³ Department of Medical Chemistry, Faculty of Medicine, Universitas Indonesia, Jakarta 10430, Indonesia

⁴ Faculty of Biology, Universitas Nasional, Jakarta 12520, Indonesia

⁵ School of Basic Pharmaceutical and Toxicological Sciences, College of Pharmacy, University of Louisiana Monroe, Monroe, LA 71201, USA

* Correspondence: rosmalena2018@gmail.com (R.R.); prasasty@ulm.edu (V.D.P.)

Abstract: Diabetes mellitus (DM) is a chronic metabolic disorder characterized by hyperglycemia, which affects multiple tissues including kidneys. Soursop leaves (*Annona muricata*) are known to have antidiabetic potential, but their molecular and cellular effects are poorly characterized. We identified the bioactive compounds in soursop leaf ethanol extract (SLEE). The SLEE substances demonstrated the total alkaloid and total flavonoid contents. Twelve bioactive compounds profiles were identified in SLEE classified as alkaloid, flavonol glycoside, and monoterpene lactone derivatives. The SLEE treatments in mice were performed by dividing Swiss Webster mice into five groups, including negative and positive controls and three experimental groups provided with SLEE (doses 150, 300, and 600 mg/kg BW) for 14 days. The mice in the experimental groups were treated with alloxan to induce diabetes. The renal samples were stained for H&E for morphological changes. However, 600 mg/kg of SLEE showed a significant effect ($p < 0.05$) on the height of the Bowman's space and prevented the tubularization of the left kidney's glomerulus ($p < 0.05$). Altogether, we report no significant difference in the glomerular diameter, the thickness of the proximal convoluted tubules, the height of the Bowman's space, and the glomerular tubularization after 14 days of treatment with SLEE.

Keywords: alloxan; *Annona muricata*; Bowman's space width; glomerular diameter; glomerular tubularization; proximal convoluted tubule



Citation: Handayani, S.I.; Sari, M.I.P.; Sardjana, M.S.; Kusmardi, K.; Nurbaya, S.; Rosmalena, R.; Sinaga, E.; Prasasty, V.D. Ameliorative Effects of *Annona muricata* Leaf Ethanol Extract on Renal Morphology of Alloxan-Induced Mice. *Appl. Sci.* **2022**, *12*, 9141. <https://doi.org/10.3390/app12189141>

Academic Editor: Monica Gallo

Received: 15 August 2022

Accepted: 9 September 2022

Published: 12 September 2022

Publisher's Note: MDPI stays neutral with regard to jurisdictional claims in published maps and institutional affiliations.



Copyright: © 2022 by the authors. Licensee MDPI, Basel, Switzerland. This article is an open access article distributed under the terms and conditions of the Creative Commons Attribution (CC BY) license (<https://creativecommons.org/licenses/by/4.0/>).

1. Introduction

Diabetes mellitus (DM) is a chronic systemic metabolic disorder characterized by hyperglycaemia and metabolic alterations [1]. DM is characterized by fasting glucose ≥ 7.0 mmol/L (126 mg/dL) or random blood glucose levels of ≥ 11.1 mmol/L (200 mg/dL) [2]. The International Diabetes Federation estimates that DM affects 415 million people worldwide, which is expected to increase to 642 million people by 2040 [3].

Renal dysfunction is a common occurrence in DM, and around 44% of new cases of chronic kidney disease are diagnosed in diabetic patients [4]. The presence of renal complications in DM patients significantly increases the mortality rates when compared with DM patients without renal complications [5,6]. However, the precise mechanism by which the renal dysfunction increases the mortality in diabetic patients remains poorly characterized [7].

Hyperglycaemia in DM can induce pathophysiological changes in the kidneys, including dysfunction of cellular responses to high glucose levels, alterations in renal vasculature, and surrounding tissues including glomeruli and podocytes [8]. Excess glucose can lead to advanced formation of glycation end (AGE) products [9,10], which bind to the basement

membrane and induce the release of pro-inflammatory cytokines, resulting in interstitial fibrosis and glomerulosclerosis [11,12]. AGE can also cause hypertrophy and excessive proliferation of cells, leading to an increase in the number and size of tubular and glomerular epithelial cells [13]. In general, DM leads to an increase in glomerular volume [14,15], along with characteristic vascular changes such as hyalinosis of the afferent and efferent arterioles and thickening of the walls of the renal arteries [16].

Currently, the management strategies of DM involve standard treatments such as insulin therapy and antidiabetic drugs [17–19]. However, these treatments have certain drawbacks, such as reduced effectiveness with oral administration, relatively short storage time, fatal side effects of hypoglycaemia due to overdosing, and discomfort due to injection needles [20]. Standard drugs also carry several other adverse side effects resulting in poor compliance by the patients [20].

Annona muricata, also known as soursop leaf, is known for its antidiabetic effects [21–24]. *A. muricata* is a plant that comes from the Annonaceae family [25]. The leaf, seed, and fruit extracts of *A. muricata* are often used in herbal medicine [26]. Those extracts from this plant inhibit glucose absorption by suppressing hydrolytic enzymes such as α -amylase and α -glucosidase [21]. Several studies have shown antihypertensive, vasodilator, anticancer, and antidepressant effects from this plant [27–29]. Moreover, Agbai and co-workers demonstrated the effect of *A. muricata* extract on the lipid profile, kidney, and liver function in a mouse model of DM induced with Streptozotocin [30]. In that study, there was a significant increase in HDL cholesterol, a reduction in serum creatinine indicating improved renal function, and reduced serum AST and ALT enzymes indicating enhanced liver function following the administration of *A. muricata* plant extract [31]. Another study by Agu et al. also showed that *A. muricata* leaf extract had an inhibitory effect on α -amylase and α -glucosidase, which outperformed the current standard antidiabetic drugs, namely acarbose and metformin [21].

However, no study has characterized a direct effect of the ethanol extract of *A. muricata* leaves on renal morphology, especially related to the proliferation and growth of the glomerulus, the Bowman's space, and the proximal tubular convolution, which are among the sites primarily affected in DM patients. We aimed to fill this gap in the literature by determining the effect of the ethanol extract of *A. muricata* leaves on renal histopathology of Swiss Webster mice with alloxan-induced diabetes.

2. Materials and Methods

The samples of this study were the kidneys of the Swiss Webster mice, which were divided into 6 groups, as listed in Table 1.

Table 1. Mice groups were treated in determining potential antidiabetic agents and doses.

| Group | Alloxan Induction | Dosage | Treatment |
|------------------|-------------------|------------------------------|----------------------|
| Normal | - | - | - |
| Negative control | 40 mg/kg BW | - | - |
| Positive control | 40 mg/kg BW | 0.65 mg/mL/day for 14 days | Glibenclamide |
| LD-SLEE * | 40 mg/kg BW | 150 mg/kg BW/day for 14 days | Soursop leaf extract |
| MD-SLEE ** | 40 mg/kg BW | 300 mg/kg BW/day for 14 days | Soursop leaf extract |
| HD-SLEE *** | 40 mg/kg BW | 600 mg/kg BW/day for 14 days | Soursop leaf extract |

* LD-SLEE = low-dose ethanol extract of soursop leaf; ** MD-SLEE = medium-dose ethanol extract of soursop leaf; *** HD-SLEE = high-dose ethanol extract of soursop leaf. BW = body weight.

2.1. *Annona Muricata* Leaf Extraction

Annona muricata leaf extraction was performed following Handayani et al. method [23]. The samples were washed and dried at room temperature. The dried simplicia of *A. muricata* leaves were ground and macerated in 70% ethanol solution overnight. Then the supernatant was separated from the precipitate and evaporated to obtain a concentrated ethanol extract of 500 g as a soursop leaf ethanol extract (SLEE). The dried SLEE of 50 mg was

dissolved in 5 ml of distilled water before it was fed to the mice models. The SLEE was screened for its phytochemical substituents, which may contribute as antioxidant agents to promote antidiabetes using qualitative analysis. Total alkaloid and flavonoid contents were determined by using colorimetric analysis.

2.2. Total Alkaloid Content Determination

The total alkaloid content (TAC) of *A. muricata* extract was determined using the method described by Lee et al. [32] with slight modification. The extracted sample was dissolved in 2 N HCl. Bromocresol green (BCG) solution with a concentration of 1×10^{-4} M was prepared by mixing 34.9 mg of BCG in 1.5 mL of 2 N sodium hydroxide (NaOH) and 2.5 mL distilled water until thoroughly dissolved and occupying up the volume to 500 mL with distilled water. The citrate–phosphate buffer (pH 4.7) was immediately prepared by stirring 2 M of disodium hydrogen phosphate (71.6 g of Na_2HPO_4 in 1 L of distilled water) and 0.2 M of citric acid (42.02 g of citric acid in 1 L of distilled water). One mL of the sample/standard solution was mixed with 5 mL of citrate–phosphate buffer solution and 5 mL of BCG indicator solution. The mixture was shaken, and 5 mL of chloroform was added then shaken vigorously after mixing. The mixture was kept at ambient temperature for 30 min. The resulting chloroform layer located in the bottom part of the sample was collected and the absorbance measured at 420 nm using a UV–vis spectrophotometer (UV-1800, Shimadzu, Japan) against a blank sample. Standard solutions of atropine in the concentration range of 0.02 mg/mL to 0.1 mg/mL were used for plotting the calibration curve $y = 0.0073x$ ($R^2 = 0.989$). All samples were analyzed in triplicate, and the content of alkaloids was expressed as mg of atropine equivalents (AE)/1 g of extract.

2.3. Total Flavonoid Content Determination

Determination of flavonoid content followed the well-established method of Zhishen et al. (1999). The flavonoid in the samples showed a yellow complex formulation with AlCl_3 solution. The color intensity was directly proportional to the flavonoid content, determined the absorbance at 510 nm. In all, 0.5 mL of quercetin solution was dissolved in methanol with 0.025, 0.050, 0.075, 0.10 and 0.15 mg/mL for 2.5 mL of distilled water, then 0.15 mL NaNO_2 5% was added. The solution was then incubated in 5 min, 0.3 mL of AlCl_3 10% was added, and it was incubated for another 5 min. Finally, 1 mL NaOH 1 M in 0.55 mL distilled water was added. The absorbance of the solution was determined at 510 nm [33].

2.4. Bioactive Compound Identification Using LC-MS/MS

An LC-MS/MS instrument (Acquity UPLC I-Class with Xevo G2-XF QToF, Waters) was used to identify the bioactive compounds contained in *A. muricata* leaf ethanol extract by injecting a sample (1 g) dissolved in distilled water and filtered by 0.45 μm filter membrane (Merck Millipore). The chromatographic separation was carried out on an ACQUITY UPLC HSS T3 column (100 mm \times 2.1 mm, 1.8 μm , Waters) at 40 °C and a flow rate of 0.5 mL/min after injecting 5 μL of SLEE. The mobile phase consisted of solvent A (distilled water and 0.1% formic acid) and solvent B (acetonitrile and 0.1% formic acid). The elution gradient was set as 97% solvent A for 0–3 min; 3%–100% linear gradient solvent B for 3–6 min; 100%–3% solvent B for 6–10 min; 97% solvent A for 10–14 min. Acetonitrile was used as a mobile phase, and the process was set within 10–40 V. Data acquisition and analysis relied on UNIFI V1.71 software (Waters), and the peaks of bioactive compounds separated by LC system were identified by profiling against the scientific database of UNIFI V1.71 [34].

2.5. Animal Model Characteristics

Mice blood samples were taken from the tails before and after alloxan administration. Mice blood samples were also taken on day 1, day 7, and day 14 after given the extracts. In addition, kidney tissue was taken after the euthanasia of all experimental animals. Renal organ tissue analyzed from 25 male Swiss Webster mice (bodyweight of 20–30 g, 12–14 old weeks) were given alloxan induction. The mice used as the research were adapted

and treated at the Animal Laboratory of the Indonesian Ministry of Health Research and Development Center at 25 °C with solar lighting for 12 h. All mice were fed and given water ad libitum. Swiss Webster male mice were treated once a day for 14 days. The mice chosen were healthy mice that seemed active and had normal blood sugar levels. The data were obtained from the histopathological observations of the kidneys of Swiss Webster mice.

2.6. Preparation of Histopathological Tissue

Renal tissue was taken at the end of day 14 and euthanasia was performed in mice by giving them the xylazine 10 mg/kg and ketamine 75–100 mg/kg using a 23–26 G syringe. The kidney tissue that has been taken was fixed using a buffer solution of 10% formalin for 24 h at room temperature. The renal tissue was sliced into smaller pieces to be put into a tissue cassette, thus tissue dehydration can be processed. The dehydration process was carried out using gradient alcohol concentration, starting from 70%, 80%, 90%, and 96%, which was administered every 2 h. The renal tissue was cleaned to remove alcohol and replace it with clearing agent as an intermediate solvent that is fully miscible with both alcohol and paraffin. The microscope slides were put in xylol to remove paraffin from dried microscope slides before staining and mounting with a coverslip. Tissue was dipped into xylol II for ½-1 h to remove all the dehydration reagent fluid or alcohol from the tissue. The tissue was then soaked in liquid paraffin for about ½ h in the oven. Once it was completed, renal tissue was then immersed in paraffin (paraplast I) for 2 h; then, it was transferred into paraffin (paraplast II) for 1 h. Next, the tissue was inserted into paraffin (paraplast III) for 2 h [35].

Furthermore, the casting process was carried out by pouring sufficient paraffin liquid into a mold made of plastic or an L-shaped metal plate (Leuckhart). Then, the heated tissue was immediately inserted using tweezers so that the paraffin would not freeze. Next, the tissue was placed into the mold and the paraffin liquid was poured to cover the entire mold. During the casting process (blocking), a mold made of plastic and metal edges was placed on the hot plate. The cube pieces of kidney tissue were cut into pieces with a thickness of 3 µm, and paraffin tape was placed on the surface of warm water at 45–50 °C.

2.7. Hematoxylin and Eosin Staining

Renal tissues that had been soaked in formalin solution were cut to a thickness of 0.3–0.5 mm. The tissues were put into a machine to be dehydrated and vacuumed. Liquid paraffin was poured on top of the tissues. The paraffin blocks or frozen sections were cut to a thickness of 3–5 µm and placed on an object glass that was smeared with adhesive. Slides were soaked in xylol (I, II and III) to remove the attached paraffin, followed by ethanol (90%, 75% and 70% consecutively) to remove the remaining xylol, then rinsed with water. Slides were stained in hematoxylin solution, rinsed with water, soaked in lithium carbonate solution, rinsed with water and stained in eosin solution. Slides were dehydrated by soaking them in ethanol (70%, 75% and 90% consecutively) and xylol (I, II and III). One drop of adhesive liquid was added and slides were covered with cover glass [22].

2.8. Image Acquisition

Analysis of blinded histopathology for renal tissues was carried out by two pathologists and the results were averaged. Histopathological readings were carried out using a light microscope directly connected to the camera with a 400× magnification that in turn was connected to a computer system. Histopathological measurements were performed using MImageView software. Each preparation was observed by looking at ten fields of view. At each field of view, a picture was taken of glomerular diameter, Bowman's space, glomerular tubularization, and proximal tubule, with the formula as follow:

$$\text{Histological score} = \sum p_i \times i$$

2.9. Statistical Analysis

The result data were analyzed using the Shapiro–Wilk test. Furthermore, a homogeneity test was carried out using Levene’s test with a p -value < 0.05 , indicating that at least the two groups had significantly different variants. In addition, bivariate analysis was performed to determine the relationship between the control and test groups on glomerular diameter, Bowman’s space width, glomerular tubularization, and proximal tubular thickness of alloxan-induced mice.

Furthermore, the data that have been obtained will be tested using an unpaired numerical comparative test. If the normal data distribution and variance results were the same, the bivariate test was a one-way ANOVA with a Bonferroni test. However, if the results of the normal data distribution and variants are different, then the test used was a one-way ANOVA with a Tamhane’s test. The post hoc test was only performed if there was a significant difference ($p < 0.05$). If ANOVA test did not meet the requirements, nonparametric analysis was performed using Mann–Whitney test.

3. Results

In this study, we exhibited an ethanolic extraction of *A. muricata* leaves. Our findings denoted that the ethanol extract of *A. muricata* leaf has concentration of alkaloids and flavonoids were 21.37 ± 3.6 μg atropine eq/mL and 43.15 ± 2.04 μg quercetin eq/mL, respectively (Figure 1). These results amplify the HPLC-ESI-MS/MS analysis, which identified various alkaloid and flavonoid compounds in this plant extract (Figure 2 and Table 2). Some common bioactive compounds were shown in the ethanolic extract, such as anonaine, chlorogenic acid, coclaurine, isolaurine, isoquercetin, kaempferol, loliolide, norcorydine, quercetin, reticuline, rutin, and xylopine (Figure 3).

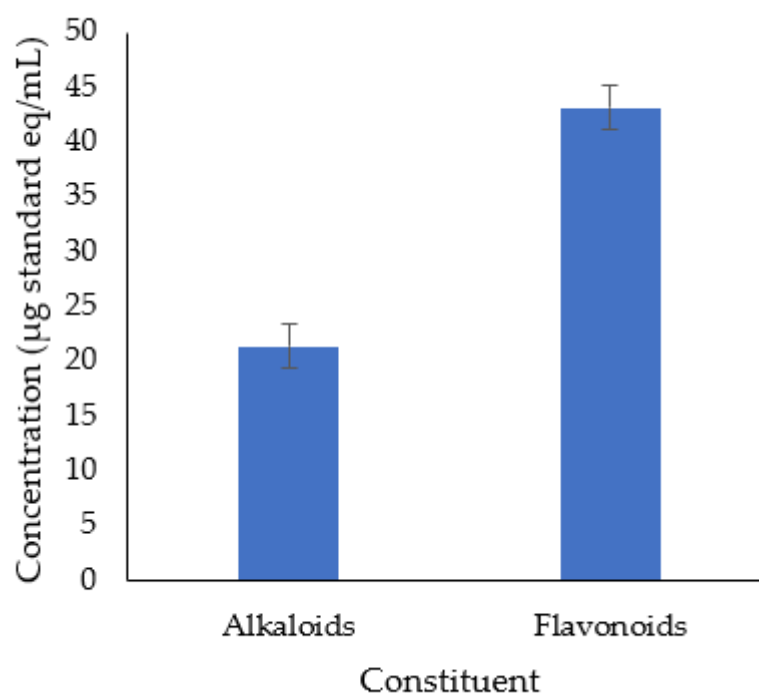


Figure 1. Alkaloids and flavonoids content in *A. muricata* leaf ethanol extract.

The diameter of renal glomeruli was significantly higher in the positive controls when compared to negative controls ($p > 0.05$, indicated normal data distribution). However, treatment with SLEE significantly reduced the glomerular diameter to the normal distribution values (Table 3).

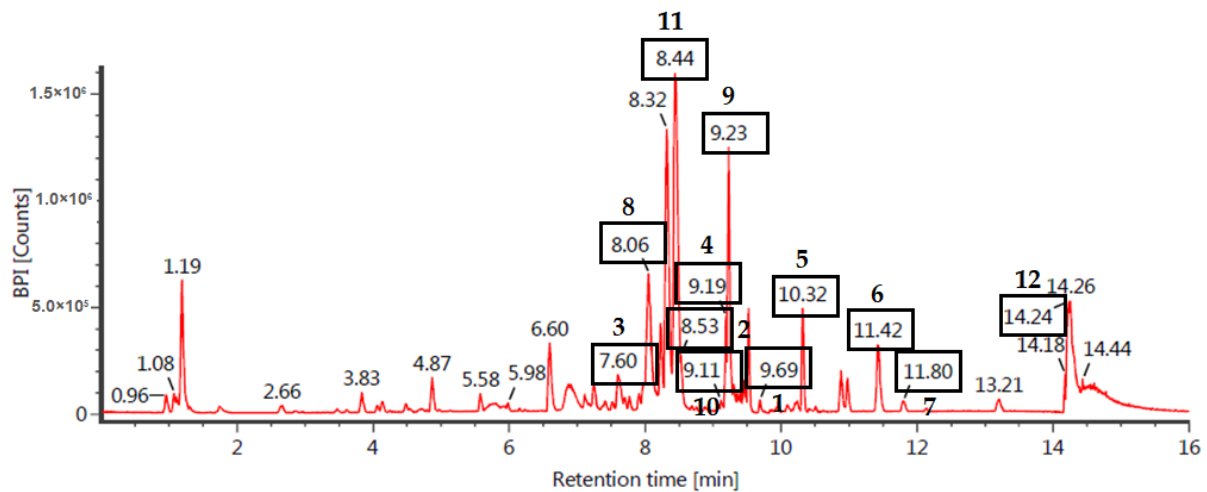


Figure 2. Chromatogram profile of bioactive compounds from *A. muricata* leaf ethanol extract using LC-MS/MS analysis.

Table 2. Bioactive compound profiles from *A. muricata* leaf ethanol extracts identified by LC-MS/MS.

| No. | Bioactive Compound | Molecular Formula | Retention Time (min) | Observed m/z | Class * |
|-----|--------------------|---|----------------------|--------------|---------|
| 1 | Anonaine | C ₁₇ H ₁₅ NO ₂ | 9.69 | 2.661.173 | AL |
| 2 | Chlorogenic acid | C ₁₆ H ₁₈ O ₉ | 8.53 | 3.551.019 | FG |
| 3 | Coclaurine | C ₁₇ H ₁₉ NO ₃ | 7.60 | 2.861.434 | AL |
| 4 | Isolaureline | C ₁₉ H ₁₉ NO ₃ | 9.19 | 3.101.433 | AL |
| 5 | Isoquercetin | C ₂₁ H ₂₀ O ₁₂ | 10.32 | 4.651.024 | FG |
| 6 | Kaempferol | C ₁₅ H ₁₀ O ₆ | 11.42 | 2.870.547 | FG |
| 7 | Loliolide | C ₁₁ H ₁₆ O ₃ | 11.80 | 1.971.172 | ML |
| 8 | Norcorydine | C ₁₉ H ₂₁ NO ₄ | 8.06 | 3.281.539 | AL |
| 9 | Quercetin | C ₁₅ H ₁₀ O ₇ | 9.23 | 3.030.496 | FG |
| 10 | Reticuline | C ₁₉ H ₂₃ NO ₄ | 9.11 | 3.301.696 | AL |
| 11 | Rutin | C ₂₇ H ₃₀ O ₁₆ | 8.44 | 6.111.601 | FG |
| 12 | Xylopin | C ₁₈ H ₁₇ NO ₃ | 14.24 | 2.961.279 | AL |

* AL: alkaloid; FG: flavonol glycoside; ML: monoterpenoid lactone.

Table 3. The overall analysis of the data distribution from all variables of left and right kidneys in the treatment mice groups.

| Variable | Treatment Group | Mean ± SE ** | p-Value |
|---|------------------|----------------|---------|
| Diameter of the renal glomerulus in the left kidney | Negative control | 594.61 ± 37.58 | 0.735 * |
| | Positive control | 608.93 ± 27.09 | 0.059 * |
| | LD-SLEE | 581.72 ± 35.41 | 0.971 * |
| | MD-SLEE | 578.64 ± 46.44 | 1.000 * |
| | HD-SLEE | 569.35 ± 32.71 | 0.915 * |
| Diameter of renal glomerulus in the right kidney | Negative control | 525.45 ± 51.29 | 0.029 |
| | Positive control | 531.10 ± 19.31 | 0.757 * |
| | LD-SLEE | 560.22 ± 29.57 | 0.409 * |
| | MD-SLEE | 546.86 ± 36.02 | 0.964 * |
| | HD-SLEE | 528.29 ± 36.15 | 0.489 * |
| Left kidney Bowman's space width | Negative control | 41.17 ± 9.29 | 0.006 |
| | Positive control | 53.86 ± 4.89 | 0.641 * |
| | LD-SLEE | 36.53 ± 7.39 | 0.176 * |
| | MD-SLEE | 46.97 ± 6.54 | 0.229 * |
| | HD-SLEE | 62.31 ± 5.53 | 0.447 * |

Table 3. Cont.

| Variable | Treatment Group | Mean \pm SE ** | <i>p</i> -Value |
|---|------------------|--------------------|-----------------|
| Right kidney Bowman's space width | Negative control | 37.33 \pm 4.02 | 0.426 * |
| | Positive control | 68.57 \pm 7.23 | 0.538 * |
| | LD-SLEE | 80.75 \pm 16.77 | 0.540 * |
| | MD-SLEE | 93.46 \pm 18.89 | 0.231 * |
| | HD-SLEE | 102.60 \pm 14.41 | 0.540 * |
| Thickness of the proximal convoluted tubule of left kidney | Negative control | 54.32 \pm 2.19 | 0.134 * |
| | Positive control | 56.23 \pm 4.85 | 0.826 * |
| | LD-SLEE | 64.13 \pm 3.19 | 0.449 * |
| | MD-SLEE | 62.24 \pm 1.94 | 0.351 * |
| | HD-SLEE | 54.01 \pm 3.15 | 0.718 * |
| The thickness of the proximal convoluted tubule of the right kidney | Negative control | 59.22 \pm 1.55 | 0.291 * |
| | Positive control | 55.37 \pm 2.98 | 0.436 * |
| | LD-SLEE | 58.48 \pm 1.65 | 0.268 * |
| | MD-SLEE | 52.87 \pm 5.82 | 0.123 * |
| | HD-SLEE | 47.33 \pm 5.40 | 0.761 * |
| Left renal glomerular tubularization | Negative control | 23.80 \pm 1.77 | 0.057 * |
| | Positive control | 13.20 \pm 1.14 | 0.090 * |
| | LD-SLEE | 17.60 \pm 1.60 | 0.377 * |
| | MD-SLEE | 15.00 \pm 1.81 | 0.627 * |
| | HD-SLEE | 9.20 \pm 3.32 | 0.808 * |
| Right renal glomerular tubularization | Negative control | 26.40 \pm 1.40 | 0.032 |
| | Positive control | 18.20 \pm 3.27 | 0.363 * |
| | LD-SLEE | 24.00 \pm 3.42 | 0.587 * |
| | MD-SLEE | 17.80 \pm 1.35 | 0.492 * |
| | HD-SLEE | 13.00 \pm 5.18 | 0.283 * |

** SE: standard error; * $p > 0.05$ indicated normal data distribution. LD-SLEE = low-dose ethanol extract of soursop leaf; MD-SLEE = medium-dose ethanol extract of soursop leaf; HD-SLEE = high-dose ethanol extract of soursop leaf.

Based on Table 3, the p -value > 0.05 were found in most treatment groups. It indicated that the experimental data were normally distributed. The p -value of Bowman's space width of left kidney were > 0.05 in positive control, low-dose ethanol extract of soursop leaf (LD-SLEE), medium-dose ethanol extract of soursop leaf (MD-SLEE), and high-dose ethanol extract of soursop leaf (HD-SLEE) groups. It indicated that these treatment groups have a normal data distribution. However, the negative control group had an abnormal data distribution with a p -value of 0.006 ($p < 0.05$).

The histopathology analyses of renal glomerular diameters, Bowman's space width, the thickness of proximal convoluted tubule, and renal glomerular tubularization of both left and right kidneys were performed by Hematoxylin and Eosin (H&E) staining at 400 \times magnification under light microscopy, as depicted in Figure 4.

The analysis of the data distribution using Shapiro–Wilk test showed a p -value > 0.05 in each treatment group of Bowman's space width of the right kidney. It showed that the distribution of data in each group of Bowman's space width of right kidney is normally distributed (Table 4).

Levene's test was used to perform data variant homogeneity of a diameter of renal glomerulus in left kidney had a p -value of 0.794 ($p > 0.05$), indicating that the data variant was homogeneous. The results of Kruskal–Wallis test from right kidney glomerular diameter had a p -value of 0.917 ($p > 0.05$), showing no significant difference in the mean between treatment groups. Therefore, Mann–Whitney post hoc test was not performed.

The results of Kruskal–Wallis test from Bowman's space width of left kidney had a p -value of 0.072 ($p > 0.05$), which showed no significant difference in the mean between the treatment groups. Thus, Mann–Whitney post hoc test was not performed. Meanwhile, Levene's test results from Bowman's space width of right kidney had a p -value of 0.319 ($p > 0.05$) in each treatment group, showing that data variance in each treatment group was homogeneous.

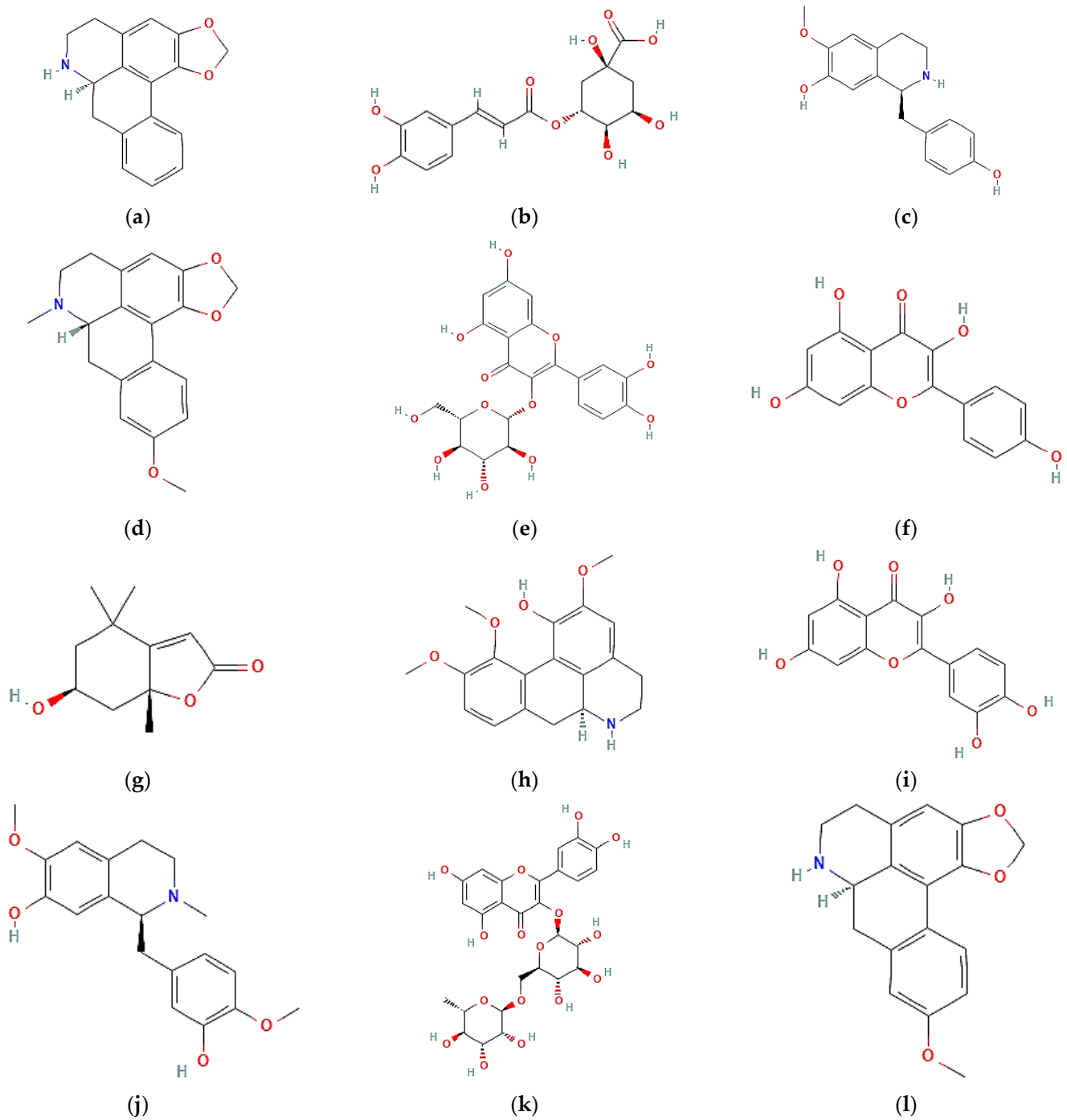


Figure 3. Bioactive compound structures found in *A. muricata* leaf ethanol extract: (a) anonaine; (b) chlorogenic acid; (c) coclaurine; (d) isolaureline; (e) isoquercetin; (f) kaempferol, (g) loliolide; (h) norcorydine; (i) quercetin; (j) reticuline; (k) rutin; (l) xylopine.

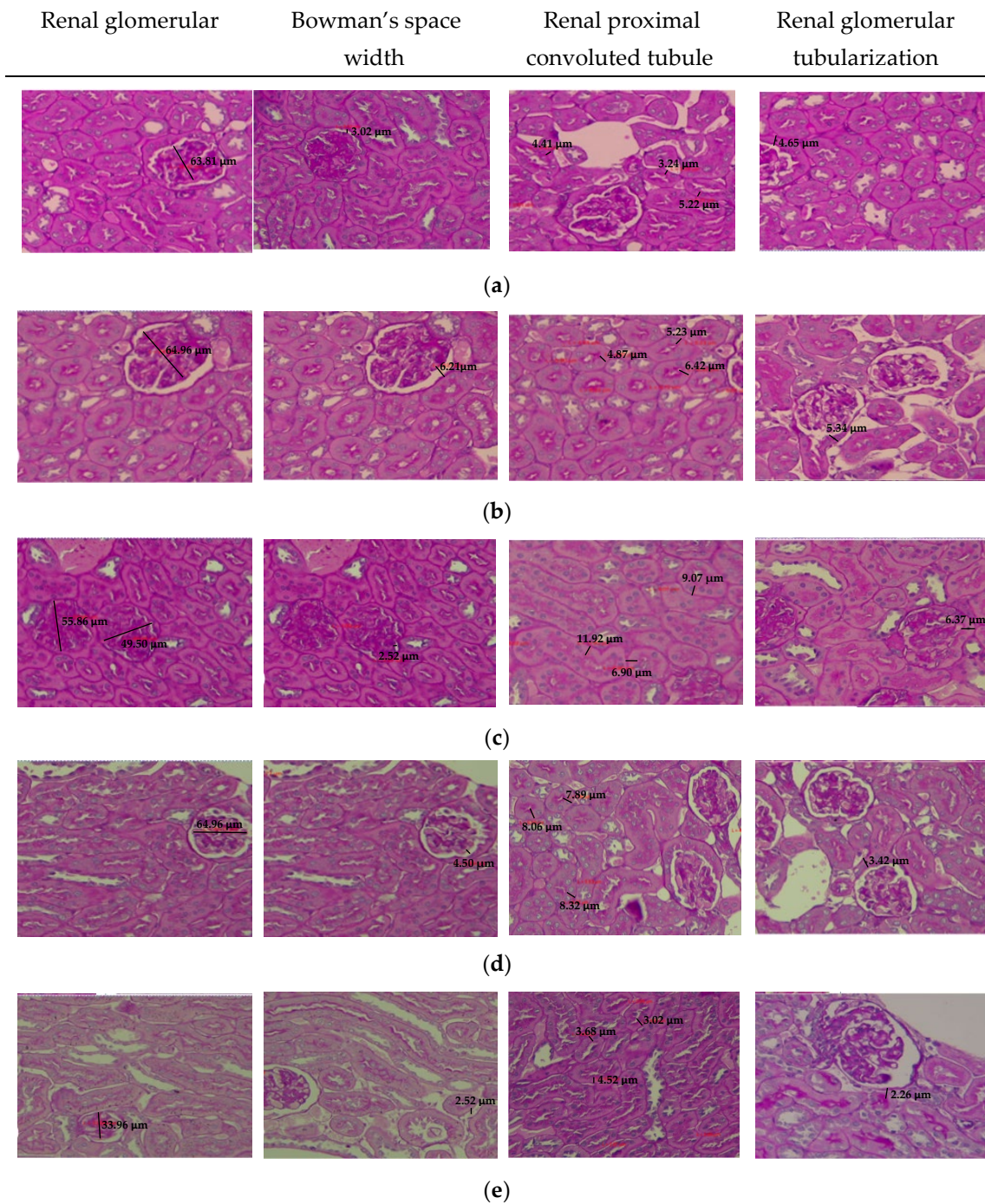


Figure 4. Histopathology profiles: the renal glomerular diameters, the Bowman's space width, the renal proximal convoluted tubule and the renal glomerular tubularization of the left kidney. All figures were prepared by Hematoxylin and Eosin (H&E) staining at 400× magnification in each group of: (a). Negative control; (b). Positive control; (c). Low-dose ethanol extract of soursop leaf (LD-SLEE) group 150 mg/kg BW; (d). Medium-dose ethanol extract of soursop leaf (MD-SLEE) group 300 mg/kg BW; (e). High-dose ethanol extract of soursop leaf (HD-SLEE) group 600 mg/kg BW.

Table 4. The homogeneity test results of data variants with Levene’s test and Kruskal–Wallis test from all left and right kidneys variables in the treatment mice groups.

| Variable | Statistical Test | Statistical Value | p-Value |
|---|---------------------|-------------------|----------|
| Diameter of renal glomerulus in the left kidney | Levene’s test | 0.418 | 0.794 * |
| Diameter of renal glomerulus in the right kidney | Kruskal–Wallis test | 0.953 | 0.917 ** |
| Left kidney Bowman’s space width | Kruskal–Wallis test | 8.603 | 0.072 ** |
| Right kidney Bowman’s space width | Levene’s test | 1.259 | 0.319 * |
| Thickness of the proximal convoluted tubule of left kidney | Levene’s test | 1.765 | 0.175 * |
| Thickness of the proximal convoluted tubule of right kidney | Levene’s test | 7.184 | 0.001 |
| Left renal glomerular tubularization | Levene’s test | 2.551 | 0.071 * |
| Right renal glomerular tubularization | Kruskal–Wallis test | 8.191 | 0.085 ** |

* $p > 0.05$ showed a homogeneous data variant in Levene’s test, and ** $p > 0.05$ indicated no significant difference in Kruskal–Wallis test.

An analysis using Levene’s test of the variable of the thickness of proximal convoluted tubule of left kidney showed a p -value of 0.175 ($p > 0.05$). Thus, the data variants in the treatment group were homogeneous. On the other hand, Levene’s test of the thickness of proximal convoluted tubule of right kidney variable had a p -value of 0.001 ($p < 0.05$) in each treatment group. It was confirmed that the data variants of proximal convoluted tubule’s thickness were significantly different from the thickness of proximal convoluted tubule of right kidney.

The data variant analysis of left renal glomerular tubularization variable using Levene’s test showed a p -value was 0.071 ($p > 0.05$). It indicated that the data variant of each treatment group was homogeneous. Moreover, the data variant analysis of right renal glomerular tubularization variable using Kruskal–Wallis test showed a p -value was 0.085 ($p > 0.05$), performing no significant difference among the treatment groups. Therefore, Mann–Whitney post hoc test was unnecessary.

Statistical analysis using the one-way ANOVA test was carried out to determine the optimal dose of soursop leaf ethanol extract (*Annona muricata*) against renal histopathological changes, particularly the thickness in right Bowman’s space width and left renal glomerular diameter of alloxan-induced mice. The one-way ANOVA statistical analysis of Bowman’s space width of right kidney and glomerular diameter of left kidney is shown in Figure 5.

Based on the one-way ANOVA test results, the thickness of left renal had a p -value of 0.947 ($p > 0.05$). It exhibited that the mean of thickness of left kidney glomerulus between treatment groups was not significantly different.

The one-way ANOVA test for the thickness of Bowman’s space width of right kidney had a p -value of 0.025 ($p < 0.05$). Furthermore, Bonferroni post hoc test was carried out, and there was a significant difference between the high-dose SLEE (HD-SLEE) group and the negative control group (Figure 2). Therefore, it was concluded that the mean of Bowman’s space width of right kidney in each group was significantly different.

The one-way ANOVA test from the thickness of proximal convoluted tubule of left kidney variable showed that a p -value was 0.119 ($p > 0.05$) and exhibited no significant difference. In contrast, the results of one-way ANOVA test for the thickness of proximal convoluted tubule of right kidney had a p -value of 0.239 ($p > 0.05$). Thus, it can be suggested that the mean of the thickness of proximal convoluted tubule of right kidney in each group was not significantly different.

The results of the data distribution that were normally distributed and the variants of the homogeneous data in each treatment group had fulfilled the one-way ANOVA test requirements. Left renal glomerular tubularization variable showed a p -value of 0.001 ($p < 0.05$), which was significantly different.

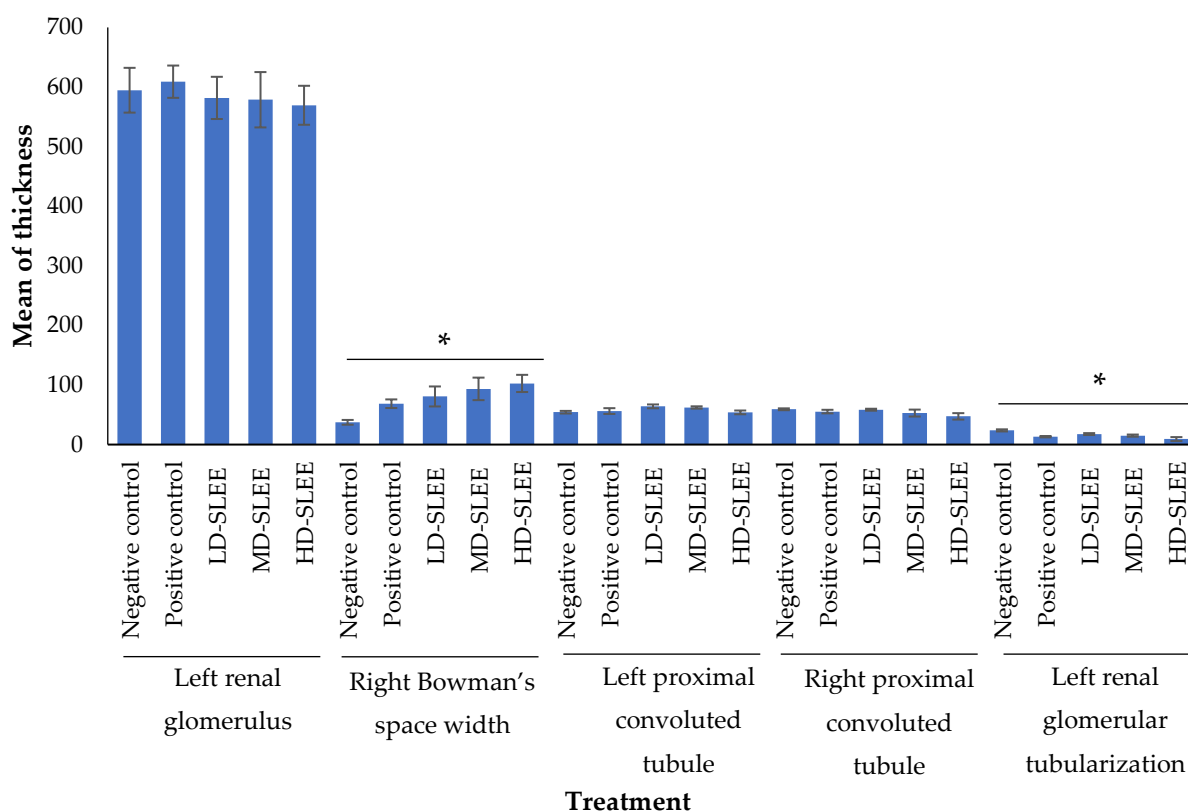


Figure 5. One-way ANOVA test results from some variables of left and right kidneys in the treatment mice groups. * $p < 0.05$ indicated significantly different results. LD-SLEE = low-dose ethanol extract of soursop leaf; MD-SLEE = medium-dose ethanol extract of soursop leaf; HD-SLEE = high-dose ethanol extract of soursop leaf.

4. Discussion

To our knowledge, no study has previously revealed the effect of soursop leaf ethanol extract (*Annona muricata*) on the glomerular diameter in a Swiss Webster mice model of DM. We compared the effects of *A. muricata* leaf aqueous extract on the glomerular diameter in Wistar rats induced by a diet of high-fat and high-fructose (dyslipidemia condition). In contrast to our findings, Nurhardiyanti reported a reduction in the glomerular diameter of the right kidney following the administration of water extract of *A. muricata* leaves (200 mg/kg BW and 400 mg/kg BW) in Wistar rats with DM [36]. Dyslipidemia is a lipid metabolism disorder characterized by increased total cholesterol, LDL, triglycerides, and reduced HDL levels. DM is a common cause of dyslipidemia [37]. Our findings are different from the research conducted by Handani et al., which examined the effects of other herbs, cowpea (*Vigna unguiculata*), on the microscopic features of diabetic kidneys. They found an improvement in the diameter of the glomerulus in diabetic mice. These effects may partly be due to antioxidant activities of vitamins C and E, which are also found in *A. muricata* [38].

The antioxidant effect in *A. muricata* leaves can neutralize cellular oxidative stress in DM, which may lead to improved renal morphology [39,40]. Thus, the increased oxidative stress in renal cells in DM can pathologically expand glomerular diameter [25,41].

We examined several changes in renal morphology, including Bowman's space width of Swiss Webster mice with DM, following the administration of ethanol extract of *A. muricata* leaves. Previous studies show that the ethanol extract of *A. muricata* leaf has antidiabetes potential [24,42]. The alterations in renal morphology, in particular a narrowing of Bowman's space width and a decrease in the necrotized renal glomerular in DM rats, are a sign of kidney structure refinement [43]. Treatment with ethanolic extract of *A. muricata* showed improvement in diabetic rats. *A. muricata* leaf ethanolic extract is considered a

source of bioactive compounds with potential health benefits. The alkaloid compound derivatives such as anonaine, coclaurine, isolaureline, norcorydune, reticuline, and xylopine may contribute as antioxidants. Similarly, flavonoid derivatives such as chlorogenic acid, isoquercetin, kaempferol, quercetin and rutin may have potential antioxidant activities. Terpene derivatives of some parts of soursop plants are effective as an antioxidant. It is also known to have antimicrobial and antitumor activities [28].

Hyperglycemia relates to an overproduction of ROS, which damages the mitochondria, causing cell death [39]. Oxidative stress due to excessive production of ROS can induce pathological alterations in renal morphology by narrowing Bowman's space width [44]. The SLEE treatment showed a reduction of Bowman's space width and this treatment dose is potential for repairing the damage in diabetic-induced mice. Some studies showed that a dose-dependent manner of *A. muricata* extract enhanced the repairment of diabetic rodents [45–47]. This is due to the role of antioxidant substances in *A. muricata* extracts, such as catalase and superoxide dismutase, and non-enzymatic antioxidants such as vitamins C and vitamin E [25,41]. The antioxidant activity of *A. muricata* can suppress ROS formation [25,41,44]. Therefore, *A. muricata* leaf extract is expected to prevent complications of DM, in particular renal damage as in diabetic nephropathy, which is characterized by changes in kidney morphology, including narrowing of Bowman's space width [25,41,44].

Proximal convoluted tubule (PCT) plays a role in the reabsorption of urine. Under normal conditions, approximately 97% of glucose is reabsorbed in the PCT [48]. The administration of a dose-dependent manner of *A. muricata* extract in alloxan-induced mice performed a refinement on the thickness of the PCT of left and right renal in this study. A study conducted on knock-out mice found that the sodium-glucose co-transporter 2 (SGLT2) is responsible for glucose reabsorption, especially in the initial segment of the PCT. In addition, sodium-glucose co-transporter1 (SGLT1) was responsible for glucose reabsorption of approximately 40% in subsequent segments in the PCT. Studies conducted on Zucker rats (in obesity-induced diabetes) found an increase in the expression of SGLT1 and SGLT2, which are primarily responsible for glucose reabsorption in the proximal tubular convolution [48]. The early onset of DM is characterized by cellular proliferation, hypertrophy, and aging of tubular cells in the PCT. The hyperglycemia condition in DM also induces structural changes in the PCT, including the thickening of the PCT due to an increase in the reabsorption capacity of proximal contours [49,50].

A normal distribution of left renal glomerular tubularization was reported in this study. This is a novel finding since no studies have previously examined the effect of ethanol extract of *A. muricata* leaves on glomerular tubularization in Swiss Webster mice treated with alloxan. Glomerular tubularization is a critical indicator for determining the severity of kidney damage [51]. Glomerular tubularization is the retrograde growth or proliferation of PCT cells around Bowman's luminal surface [52].

The ethanol extract of *A. muricata* leaves is expected to prevent glomerular tubularization in DM, as this extract lowered the blood glucose and lipid levels in alloxan-induced Wistar rats [53]. The ethanol extract of *A. muricata* leaves contains several active substances that have the antidiabetes and antioxidant potential. *A. muricata* leaves contain phenolics, catechine, epicatechin, routine, other flavonoid glycosides, and chlorogenic acid, which are known to have antioxidant effects. The antioxidant activity of *A. muricata* leaves can suppress the production of ROS and reduce oxidative stress, which is a major cause of the renal damage in DM characterized by alterations in renal morphology and glomerular tubularization [25,39,41,44].

5. Conclusions

Altogether, we reported that soursop leaf ethanol extracts (SLEE) have substances of total alkaloid and total flavonoid contents. Twelve bioactive compounds profiles were identified in the SLEE classified as alkaloid, flavonol glycoside, and monoterpenoid lactone derivatives, which have an antioxidant effect that scavenges the excessive reactive oxygen species (ROS). There is a significant difference in Bowman's space width of alloxan-induced

mice after administration of the SLEE. Renal glomerular tubularization of alloxan-induced mice was reduced following the administration of the SLEE at a dose-dependent manner. Taken together, our results indicate a therapeutic potential of *A. muricata* in kidney restoration in DM. Further studies are required to dissect the molecular, cellular, and functional effects of *A. muricata* on diabetic kidneys.

Author Contributions: Conceptualization, S.I.H., M.S.S. and M.I.P.S.; methodology, S.I.H., M.I.P.S., K.K., V.D.P. and R.R.; software, S.I.H., M.I.P.S. and V.D.P.; validation, S.I.H., M.I.P.S., K.K., V.D.P., R.R., S.N. and M.S.S.; formal analysis, S.I.H., M.I.P.S., S.N. and V.D.P.; investigation, S.I.H., M.I.P.S., E.S. and V.D.P.; resources, S.I.H.; data curation, S.I.H. and M.I.P.S.; writing—original draft preparation, S.I.H. and M.I.P.S.; writing—review and editing, S.I.H., M.I.P.S., E.S., K.K., V.D.P., R.R., S.N. and M.S.S.; visualization, S.I.H., M.I.P.S. and V.D.P.; supervision, S.I.H.; project administration, S.I.H.; funding acquisition, S.I.H. All authors have read and agreed to the published version of the manuscript.

Funding: This research was supported by a PUTI research grant with the grant number: NKB-3507/UN2.RST/HKP.0500/2020.

Institutional Review Board Statement: The Research Ethics Committee approved all the experimental protocols with mice models at the Faculty of Medicine, Universitas Indonesia (KET.373/UN2.F1/ETIK/PPM.00.02/2019).

Informed Consent Statement: Not applicable.

Data Availability Statement: Data supporting reported results are included in this article. All plant samples are available from the authors.

Acknowledgments: We would like to thank the Director of Research and Public Services Universitas Indonesia for valuable supports.

Conflicts of Interest: The authors declare no conflict of interest.

References

- Vieira, R.; Souto, S.B.; Sánchez-López, E.; López Machado, A.; Severino, P.; Jose, S.; Santini, A.; Silva, A.M.; Fortuna, A.; García, M.L. Sugar-Lowering Drugs for Type 2 Diabetes Mellitus and Metabolic Syndrome—Strategies for in Vivo Administration: Part-2. *J. Clin. Med.* **2019**, *8*, 1332. [[CrossRef](#)] [[PubMed](#)]
- Jeon, J.Y.; Ko, S.-H.; Kwon, H.-S.; Kim, N.H.; Kim, J.H.; Kim, C.S.; Song, K.-H.; Won, J.C.; Lim, S.; Choi, S.H. Prevalence of Diabetes and Prediabetes According to Fasting Plasma Glucose and HbA1c. *Diabetes Metab. J.* **2013**, *37*, 349. [[CrossRef](#)] [[PubMed](#)]
- Al-Lawati, J.A. Diabetes Mellitus: A Local and Global Public Health Emergency! *Oman Med. J.* **2017**, *32*, 177. [[CrossRef](#)] [[PubMed](#)]
- Mihardja, L.; Delima, D.; Massie, R.G.; Karyana, M.; Nugroho, P.; Yunir, E. Prevalence of Kidney Dysfunction in Diabetes Mellitus and Associated Risk Factors among Productive Age Indonesian. *J. Diabetes Metab. Disord.* **2018**, *17*, 53–61. [[CrossRef](#)]
- Fox, C.S.; Matsushita, K.; Woodward, M.; Bilo, H.J.; Chalmers, J.; Heerspink, H.J.L.; Lee, B.J.; Perkins, R.M.; Rossing, P.; Sairenchi, T. Associations of Kidney Disease Measures with Mortality and End-Stage Renal Disease in Individuals with and without Diabetes: A Meta-Analysis. *Lancet* **2012**, *380*, 1662–1673. [[CrossRef](#)]
- DiGangi, C. Neutrophil-Lymphocyte Ratio: Predicting Cardiovascular and Renal Complications in Patients with Diabetes. *J. Am. Assoc. Nurse Pract.* **2016**, *28*, 410–414. [[CrossRef](#)]
- Gregg, E.W.; Sattar, N.; Ali, M.K. The Changing Face of Diabetes Complications. *Lancet Diabetes Endocrinol.* **2016**, *4*, 537–547. [[CrossRef](#)]
- Reidy, K.; Kang, H.M.; Hostetter, T.; Susztak, K. Molecular Mechanisms of Diabetic Kidney Disease. *J. Clin. Investig.* **2014**, *124*, 2333–2340. [[CrossRef](#)]
- Vlassara, H.; Uribarri, J. Advanced Glycation End Products (Age) and Diabetes: Cause, Effect, or Both? *Curr. Diab. Rep.* **2014**, *14*, 453. [[CrossRef](#)]
- Aragno, M.; Mastrocola, R. Dietary Sugars and Endogenous Formation of Advanced Glycation Endproducts: Emerging Mechanisms of Disease. *Nutrients.* **2017**, *9*, 385. [[CrossRef](#)]
- Pasupulati, A.K.; Chitra, P.S.; Reddy, G.B. Advanced Glycation End Products Mediated Cellular and Molecular Events in the Pathology of Diabetic Nephropathy. *Biomol. Concepts.* **2016**, *7*, 293–309. [[CrossRef](#)]
- Jourde-Chiche, N.; Fakhouri, F.; Dou, L.; Bellien, J.; Burtey, S.; Frimat, M.; Jarrot, P.-A.; Kaplanski, G.; Le Quintrec, M.; Pernin, V. Endothelium Structure and Function in Kidney Health and Disease. *Nat. Rev. Nephrol.* **2019**, *15*, 87–108. [[CrossRef](#)]
- Romagnani, P.; Remuzzi, G.; Glassock, R.; Levin, A.; Jager, K.J.; Tonelli, M.; Massy, Z.; Wanner, C.; Anders, H.-J. Chronic Kidney Disease. *Nat. Rev. Dis. Primers.* **2017**, *3*, 1–24. [[CrossRef](#)]
- Satoh, M.; Kobayashi, S.; Kuwabara, A.; Tomita, N.; Sasaki, T.; Kashihara, N. In Vivo Visualization of Glomerular Microcirculation and Hyperfiltration in Streptozotocin-Induced Diabetic Rats. *Microcirculation* **2010**, *17*, 103–112. [[CrossRef](#)]

15. Lee, M.M.; Brooksbank, K.J.; Wetherall, K.; Mangion, K.; Roditi, G.; Campbell, R.T.; Berry, C.; Chong, V.; Coyle, L.; Docherty, K.F. Effect of Empagliflozin on Left Ventricular Volumes in Patients with Type 2 Diabetes, or Prediabetes, and Heart Failure with Reduced Ejection Fraction (Sugar-Dm-Hf). *Circulation* **2021**, *143*, 516–525. [[CrossRef](#)]
16. Akhtar, M.; Taha, N.; Nauman, A.; Mujeeb, I.; Al-Nabet, A. Diabetic Kidney Disease: Past and Present. *Adv. Anat. Pathol.* **2020**, *27*, 87–97. [[CrossRef](#)]
17. Pandey, A.; Tripathi, P.; Pandey, R.; Srivatava, R.; Goswami, S. Alternative Therapies Useful in the Management of Diabetes: A Systematic Review. *J. Pharm. Bioallied Sci.* **2011**, *3*, 504.
18. Campbell, R.K. Type 2 Diabetes: Where We Are Today: An Overview of Disease Burden, Current Treatments, and Treatment Strategies. *J. Am. Pharm. Assoc.* **2009**, *49*, S3–S9. [[CrossRef](#)]
19. Jacobi, J.; Bircher, N.; Krinsley, J.; Agus, M.; Braithwaite, S.S.; Deutschman, C.; Freire, A.X.; Geehan, D.; Kohl, B.; Nasraway, S.A. Guidelines for the Use of an Insulin Infusion for the Management of Hyperglycemia in Critically Ill Patients. *Crit. Care Med.* **2012**, *40*, 3251–3276. [[CrossRef](#)]
20. Offurum, A.; Wagner, L.-A.; Gooden, T. Adverse Safety Events in Patients with Chronic Kidney Disease (Ckd). *Expert Opin. Drug Saf.* **2016**, *15*, 1597–1607. [[CrossRef](#)]
21. Agu, K.; Eluehike, N.; Ofeimun, R.; Abile, D.; Ideho, G.; Ogedengbe, M.; Onose, P.; Elekofehinti, O. Possible Anti-Diabetic Potentials of *Annona muricata* (Soursop): Inhibition of A-Amylase and A-Glucosidase Activities. *Clin. Phytosci.* **2019**, *5*, 21. [[CrossRef](#)]
22. Dewi, S.N.; Handayani, S.I.; Stephanie, M.; Nurbaya, S.; Prasasty, V.D. Assessment of the *Annona muricata* Leaf Ethanol Extract Effect on the Diameter of Pancreatic Islets in Alloxan-Induced Mice. *Online J. Biol. Sci.* **2020**, *20*, 50–56. [[CrossRef](#)]
23. Handayani, S.I.; Dewi, S.N.; Stephanie, M.; Nurbaya, S.; Prasasty, V.D. The Effect of *Annona muricata* Leaf Ethanol Extract on Insulin Expression and Glucagon-Like Peptide-1 Level in Alloxan-Induced Mice. *Syst. Rev. Pharm.* **2020**, *11*, 363–370.
24. Justino, A.B.; Miranda, N.C.; Franco, R.R.; Martins, M.M.; Da Silva, N.M.; Espindola, F.S. *Annona muricata* Linn. Leaf as a Source of Antioxidant Compounds with in Vitro Antidiabetic and Inhibitory Potential against A-Amylase, A-Glucosidase, Lipase, Non-Enzymatic Glycation and Lipid Peroxidation. *Biomed. Pharmacother.* **2018**, *100*, 83–92. [[CrossRef](#)] [[PubMed](#)]
25. Moghadamtousi, S.Z.; Fadaeinasab, M.; Nikzad, S.; Mohan, G.; Ali, H.M.; Kadir, H.A. *Annona muricata* (Annonaceae): A Review of Its Traditional Uses, Isolated Acetogenins and Biological Activities. *Int. J. Mol. Sci.* **2015**, *16*, 15625–15658. [[CrossRef](#)] [[PubMed](#)]
26. Patel, M.S.; Patel, J.K. A Review on a Miracle Fruits of *Annona Muricata*. *J. Pharmacogn. Phytochem.* **2016**, *5*, 137.
27. Djarot, P.; Badar, M. Formulation and Production of Granule from *Annona muricata* Fruit Juice as Antihypertensive Instant Drink. *Int. J. Pharm. Pharm. Sci.* **2017**, *9*, 18–22. [[CrossRef](#)]
28. Mishra, T. Waging Green War against Cardiovascular Ailments. *Eur. J. Biomed. Pharm.* **2018**, *5*, 192–199.
29. Pieme, C.A.; Kumar, S.G.; Dongmo, M.S.; Moukette, B.M.; Boyoum, F.F.; Ngogang, J.Y.; Saxena, A.K. Antiproliferative Activity and Induction of Apoptosis by *Annona muricata* (Annonaceae) Extract on Human Cancer Cells. *BMC Complement. Altern. Med.* **2014**, *14*, 516. [[CrossRef](#)]
30. Agbai, E.; Njoku, C.; Nwafor, A. Effect of Aqueous Extract of *Annona muricata* Seed on Atherogenicity in Streptozotocin-Induced Diabetic Rats. *Afr. J. Pharm. Pharmacol.* **2015**, *9*, 745–755. [[CrossRef](#)]
31. Kharroubi, A.T.; Darwish, H.M. Diabetes Mellitus: The Epidemic of the Century. *World J. Diabetes* **2015**, *6*, 850. [[CrossRef](#)]
32. Lee, C.H.; Lee, T.H.; Ong, P.Y.; Wong, S.L.; Hamdan, N.; Elgharrawy, A.A.; Azmi, N.A. Integrated Ultrasound-Mechanical Stirrer Technique for Extraction of Total Alkaloid Content from *Annona muricata*. *Proc. Biochem.* **2021**, *109*, 104–116. [[CrossRef](#)]
33. Zhishen, J.; Mengcheng, T.; Jianming, W. The Determination of Flavonoid Contents in Mulberry and Their Scavenging Effects on Superoxide Radicals. *Food Chem.* **1999**, *64*, 555–559. [[CrossRef](#)]
34. Lee, J.W.; Ji, S.-H.; Lee, Y.-S.; Choi, D.J.; Choi, B.-R.; Kim, G.-S.; Baek, N.-I.; Lee, D.Y. Mass Spectrometry Based Profiling and Imaging of Various Ginsenosides from Panax Ginseng Roots at Different Ages. *Int. J. Mol. Sci.* **2017**, *18*, 1114. [[CrossRef](#)]
35. Hasugian, S.A.; Lubis, K.; Doan, H.V. Profile of Histopathology of Cervical Cancer Tissues in Patients of the Dr. Pirngadi Medan Hospital. *J. Biosains.* **2020**, *6*, 90–97. [[CrossRef](#)]
36. Nurhardiyanti, S. Efek Ekstrak Air Daun Sirsak (*Annona muricata* L.) Terhadap Luas Area Kolagen Arteri Renalis Dan Diameter Glomerulus Ginjal Sinistra Tikus Wistar Model Dislipidemia. *J. Community Health.* **2019**, *7*, 43–52.
37. Aman, M.; Soewondo, P.; Soelistijo, S.; Arsana, P.; Wismandari; Zufry, H.; Rosandi, R. *Pedoman Pengelolaan Dislipidemia Di Indonesia 2019*; Pb Perkeni: Jakarta, Indonesia, 2019.
38. Florence, N.T.; Benoit, M.Z.; Jonas, K.; Alexandra, T.; Désiré, D.D.P.; Pierre, K.; Théophile, D. Antidiabetic and Antioxidant Effects of *Annona muricata* (Annonaceae), Aqueous Extract on Streptozotocin-Induced Diabetic Rats. *J. Ethnopharmacol.* **2014**, *151*, 784–790. [[CrossRef](#)]
39. Hosseini, A.; Abdollahi, M. Diabetic Neuropathy and Oxidative Stress: Therapeutic Perspectives. *Oxid. Med. Cell. Longev.* **2013**, *2013*, 168039. [[CrossRef](#)]
40. George, V.C.; Kumar, D.N.; Suresh, P.; Kumar, R.A. Antioxidant, DNA Protective Efficacy and Hplc Analysis of *Annona muricata* (Soursop) Extracts. *J. Food Sci. Technol.* **2015**, *52*, 2328–2335. [[CrossRef](#)]
41. Coria-Téllez, A.V.; Montalvo-González, E.; Yahia, E.M.; Obledo-Vázquez, E.N. *Annona muricata*: A Comprehensive Review on Its Traditional Medicinal Uses, Phytochemicals, Pharmacological Activities, Mechanisms of Action and Toxicity. *Arab. J. Chem.* **2018**, *11*, 662–691. [[CrossRef](#)]

42. Opara, P.; Enemor, V.; Eneh, F.; Emengaha, F. Blood Glucose–Lowering Potentials of *Annona muricata* Leaf Extract in Alloxan–Induced Diabetic Rats. *Eur. J. Biol. Biotechnol.* **2021**, *2*, 106–113. [[CrossRef](#)]
43. Amann, K.; Benz, K. *Structural Renal Changes in Obesity and Diabetes*; Seminars in Nephrology; Elsevier: Amsterdam, The Netherlands, 2013; pp. 23–33.
44. Sandireddy, R.; Yerra, V.G.; Areti, A.; Komirishetty, P.; Kumar, A. Neuroinflammation and Oxidative Stress in Diabetic Neuropathy: Futuristic Strategies Based on These Targets. *Int. J. Endocrinol.* **2014**, *2014*, 674987. [[CrossRef](#)]
45. Ishola, I.O.; Awodele, O.; Olusayero, A.M.; Ochieng, C.O. Mechanisms of Analgesic and Anti-Inflammatory Properties of *Annona muricata* Linn. (Annonaceae) Fruit Extract in Rodents. *J. Med. Food* **2014**, *17*, 1375–1382. [[CrossRef](#)]
46. Setiadi, R.; Zein, A.; Nauphar, D. Antihyperglycemic Effectiveness Comparison of Ethanol Extract of Soursop Leaf (*Annona muricata* L.) Againsts Acarbose in Streptozotocin-Induced Diabetic White Rats. *J. Phys. Conf. Ser.* **2019**, *1146*, 012009. [[CrossRef](#)]
47. Subaraman, M.; Gayathri, R.; Priya, V.V. In Vitro Antidiabetic Activity of Crude Acetone Leaf Extract of *Annona muricata*. *Drug Invent. Today* **2020**, *14*, 837–839.
48. Vallon, V. The Proximal Tubule in the Pathophysiology of the Diabetic Kidney. *Am. J. Physiol.-Regul. Integr. Comp. Physiol.* **2011**, *300*, R1009–R1022. [[CrossRef](#)]
49. Vallon, V.; Thomson, S. Renal Function in Diabetic Disease Models: The Tubular System in the Pathophysiology of the Diabetic Kidney. *Annu. Rev. Physiol.* **2012**, *74*, 351–375. [[CrossRef](#)]
50. Peres, G.B.; Michelacci, Y.M. The Role of Proximal Tubular Cells in the Early Stages of Diabetic Nephropathy. *J. Diabetes Metab.* **2015**, *6*, 2.
51. Stenzel, T.; Weidgang, C.; Wagner, K.; Wagner, F.; Gröger, M.; Weber, S.; Stahl, B.; Wachter, U.; Vogt, J.; Calzia, E. Association of Kidney Tissue Barrier Disrupture and Renal Dysfunction in Resuscitated Murine Septic Shock. *Shock. Inj. Inflamm. Sepsis Lab. Clin. Approaches* **2016**, *46*, 398–404. [[CrossRef](#)]
52. Isaac, J.; Tögel, F.E.; Westenfelder, C. Extent of Glomerular Tubularization Is an Indicator of the Severity of Experimental Acute Kidney Injury in Mice. *Nephron. Exp. Nephrol.* **2007**, *105*, e33–e40. [[CrossRef](#)]
53. Sovia, E.; Ratwita, W.; Wijayanti, D.; Novianty, D. Hypoglycemic and Hypolipidemic Effects of *Annona muricata* L. Leaf Ethanol Extract. *Int. J. Pharm. Pharm. Sci.* **2017**, *9*, 170–174. [[CrossRef](#)]